IEEE Access
Multidisciplinary ⋮ Rapid Review ⋮ Open Access Journal

Received 25 April 2023, accepted 12 June 2023, date of publication 15 June 2023, date of current version 22 June 2023.

Digital Object Identifier 10.1109/ACCESS.2023.3286817

RESEARCH ARTICLE

High Order Spectral Analysis of Ferroresonance Phenomena in Electric Power Systems

TAHIR CETIN AKINCI[1,2], (Senior Member, IEEE), OMER AKGUN[3], MUSA YILMAZ[4,5], (Senior Member, IEEE), AND ALFREDO A. MARTINEZ-MORALES[1,4,6]

[1]Winston Chung Global Energy Center, University of California at Riverside, Riverside, CA 92521, USA
[2]Electrical Engineering Department, Istanbul Technical University, 34469 Istanbul, Turkey
[3]Computer Engineering Department, Marmara University, 34854 Istanbul, Turkey
[4]Bourns College of Engineering, Center for Environmental Research and Technology, University of California at Riverside, Riverside, CA 92521, USA
[5]Electrical and Electronics Engineering Department, Batman University, 72000 Batman, Turkey
[6]Electrical and Computer Engineering Department, University of California at Riverside, Riverside, CA 92521, USA

Corresponding author: Tahir Cetin Akinci (tahircetin.akinci@ucr.edu)

ABSTRACT This study presents a comprehensive investigation of ferroresonance, a dangerous electrical phenomenon that poses significant financial risks. Using real electrical transmission line parameters, we simulated synthetic ferroresonance scenarios on a model and analyzed the resulting data using high-order spectral analysis methods, including the Wigner-Ville method, Welch method, frequency-power analysis, and spectral methods. Our analysis revealed changes in frequency and power before and after ferroresonance, with third and fourth-order cumulants being calculated. We confirmed the accuracy of the power transmission line's base frequency and power before the ferroresonance event and determined the frequency and power values before and after ferroresonance with frequency-power analysis. Our cumulative analysis results showed symmetrical results that are consistent with the properties of ferroresonance. Additionally, we found that the Wigner Ville method's high-resolution results were significantly more effective than conventional methods. Our study's findings provide valuable insights into ferroresonance's behavior and may inform the development of more effective prevention and mitigation strategies.

INDEX TERMS Comulant, electric power system, ferroresonance, high order spectral analysis, Wigner-Ville.

I. INTRODUCTION

The growth of industrialization has facilitated the expansion and development of electricity transmission systems in countries [1]. Energy transmission lines play a crucial role in the transmission of energy from a limited number of power plants to remote locations [2]. These systems must be efficient, economical, sustainable, and provide quality energy to justify investment in energy transmission lines [3]. The majority of power transmission line malfunctions are caused by faults in the transmission lines or in components such as line breakers and switches [4]. The timing and causes of these failures are important for preventing future incidents [4], [5], [6]. Voltage drops in the electric power network and electricity blackouts can lead to issues with devices connected to the network [7]. These problems can result in power quality issues in the system or cause significant material losses by partially or completely damaging the transmission line [8]. Even millisecond-level malfunctions can lead to prolonged power outages and labour losses [9].

The phenomenon of ferroresonance that can occur in energy power network systems is featured by overvoltage or current in the system [10]. These high amplitude voltages and currents, which are a result of a malfunction in the power system, can cause destructive and irreparable failures throughout the system in a short amount of time [11], [12]. Despite being known for many years, the causes and prevention of ferroresonance remain a mystery due to the presence

The associate editor coordinating the review of this manuscript and approving it for publication was Qingli Li.

of non-linear components in power systems, such as saturated transformers, linear and nonlinear resistors, and inductive and capacitive elements [12], [13], [14], [15], [16].

Ferroresonance refers to the occurrence of series resonance in an electrical circuit, where a non-linear inductance element involving a capacitor and a magnetizing inductance that is saturated are present [12], [7]. This phenomenon can arise in various electrical systems, including transformers, circuits, and electric power transmission lines, due to events such as sudden load failure, interruption of one phase in a three-phase transmission line, lightning strikes, or transformer issues [12], [17], [18]. The resulting waveform is asymmetrical with high amplitude, leading to destructive overvoltages throughout the system, which can impact other phases [12], [19]. Ferroresonance exhibits multiple continuous and steady-state responses under the same network parameters and can occur during transient situations. To prevent ferroresonance, it is crucial to perform a comprehensive analysis and consider all potential triggering scenarios [12].

It is also important to predict where, when, and under what conditions ferroresonance may occur [20], [21]. While efforts are being made to eliminate ferroresonance formation conditions by making smart power systems, it is estimated that electric power lines will be at a higher risk for ferroresonance in the future due to increased voltage levels and increased differences between line capacitance and transformer magnetic saturation [17], [19], [21].

The Fourier transform is not suitable for the analysis of non-stationary signals as it converts the signal into infinite waves that are not localized in time [14], [19], [22]. Therefore, two-dimensional analysis using methods such as HOSA spectral analysis is more appropriate for investigating non-stationary signals like ferroresonance [14], [18].

The use of the HOSA method used in this study in the analysis of the ferroresonance phenomena in Electric Power systems and the comparison of the superiorities of the methods for this method are listed below.

- HOSA is a very useful method for performing harmonic analysis in electrical power systems, but traditional spectral analysis methods are used more generally. Traditional methods such as FFT and DFT are used in a variety of applications such as the analysis of frequency and power spectrums.
- HOSA analysis is very successful in identifying and solving harmonic problems in electrical power systems. This method can also help detect ferroresonance phenomena by determining the ratios and frequencies of harmonics. In addition, the HOSA analysis also estimates the possible consequences of fluctuations caused by ferroresonance events.
- HOSA is optimized to isolate high frequency harmonic components and is very successful in this field. This allows HOSA to provide higher resolution and more accurate results compared to other spectral analysis methods. In this sense, it gives more precise results than traditional spectral analysis methods for ferroresonance data. HOSA is also faster compared to traditional methods such as FFT and DFT. This results in faster results when used for large datasets.
- HOSA is more resistant to noise, harmonic distortion and other power quality issues. This allows HOSA to provide more accurate results compared to other spectral analysis methods.
- HOSA does not require that the data to be analyzed is a continuous time series, in this sense, it is seen from the analyzes that it gives effective results in the analysis of Ferroresonance data. This offers a more flexible approach to sampling and recording data, as well as providing higher resolution, faster processing and better resilience.
- HOSA analysis is very successful in identifying and solving harmonic problems in electrical power systems. This method can also help detect ferroresonance phenomena by determining the ratios and frequencies of harmonics. In addition, the HOSA analysis also estimates the possible consequences of fluctuations caused by ferroresonance events.
- Conventional methods mostly use test devices for ferroresonance detection, while a separate test device is not required for HOSA analysis. This provides an advantage in terms of cost.

In this study, the phenomena of ferroresonance were studied using HOSA spectral analysis methods.

II. MATHEMATICAL BACKGROUND

High-Order Spectral Analysis (HOSA) methods contain much more information than is transmitted by auto-correlation and power in a non-stochastic Gauss or deterministic signal [23]. Includes higher-level spectra, also known as higher-level moments or cumulants of a signal with HOSA. In this sense, HOSA contains comprehensive information for high-order spectral analysis.

A. CUMULANT

Second-order statistics such as $R(\tau)$ correlation and S $(\omega) = F\ \{R(\tau)\}$ power spectral density is an effective method used in the analysis of gauss, stationary and linear processes. In the equations below, the mathematical relations of moments and deterministic signs are given. Moments provide effective results in the analysis of deterministic signals, and cumulations in random signals [6], [24].

$$m_X = E\,(X) \tag{1}$$

The first-order moment is given in Equation (1) and second-order correlation function is given in Equation (2).

$$\sigma_X^2 = E\left[(X - m_X)^2\right], m_X^2(i) = E\,\{X(n).X(n+i)\} \tag{2}$$

The auto correlation function (ACF) is a commonly used tool for analyzing Gaussian-distributed $X(n)$, stationary, and nonlinear processes. However, it is not enough to fully characterize non-Gaussian processes. In these cases, higher-order statistics (HOSA) provide better results. HOSA is obtained through the use of high-order moments, such as (m^3, m^4, ….). These high-order moments are expressed as nonlinear combinations of cumulants, (c^1, c^2, c^3, …). Equation (3) shows the equation for the third-order moment, and Equation (4) shows the equation for the fourth-degree moment.

$$m_X^3(i,j) = E\{X(n).X(n+i).X(n+j)\} \tag{3}$$

$$m_X^4(i,j,k) = E\{X(n).X(n+i).X(n+j).X(n+k)\} \tag{4}$$

Cumulating equations for the zero-average process are given in Equation (5-7).

$$c^2(i) = m(i) \tag{5}$$

$$c^3(i,j) = m(i,j) \tag{6}$$

$$c^4(i,j,k) = m^4(i,j,k) - m^2(i).m^2(j,k) - m^2(j).m^2(i,k) - m^2(k).m^2(i,j) \tag{7}$$

In Equation (8), cross cumulating expression is given for random processes [6].

$$C_{XYZ}(m,n) = E\{X(i)Y(i+m)Z(i+n)\} \tag{8}$$

In this study, the ferroresonance signal (2,1) was evaluated as the output of an ARMA process (model), and the 3rd and 4th degrees of the process were analysed.

B. WIGNER-VILLE DISTRIBUTION (WVD)

The investigation of time-frequency distributions comprises the analysis of signals in a two-dimensional time-frequency plane [25]. The Wigner-Ville Distribution (WVD) approach provides a comprehensive representation of time-frequency by characterizing the energy intensity of a signal simultaneously at different time and frequency points. Time-frequency representations can be broadly classified into two categories: second-order methods and linear approaches. Second-order methods encompass fundamental signal processing analysis, while linear approaches encompass Gabor transform, Zak transform, and wavelet transform analysis [25], [26], [27], [28]. The WVD is particularly well-suited for high-resolution analysis of non-stationary signals, offering a detailed understanding of the energy spectrum in terms of the instant power and frequency in time, as well as the total energy of the signal in the time-frequency plane [28], [29], [30], [31], [32]. The WVD of a non-stationary random signal $x(t)$ is represented by the frequency of time t, f, and lag τ and is defined by equation (9).

$$W(t,f) = \int_{-\infty}^{+\infty} x\left(t+\frac{\tau}{2}\right) + x\left(t-\frac{\tau}{2}\right) e^{-i\omega f\tau} d\tau \tag{9}$$

The distribution in the WWD is quadratic, so the implementation of WVD is limited by the presence of interference terms. These can be defined in equation (10), considering the basic mono-components $m(t)$ and $n(t)$ [30], [33], [34], [35], [36].

C. PSD WELCH METHODS

Welch's method is a widely used technique for estimating power spectral density of a signal. This method is based on periodogram analysis, which involves dividing the time series into overlapping sections to obtain an improved periodogram for each section. The Welch method then computes the power spectral density by averaging these improved periodograms. Non-rectangular windows are used to overlap and decrease the weight of samples at the end of the sections, which reduces the variance relative to a single periodogram estimate. The i'th improved periodogram is given by Equation (10) [6], [37], [38].

$$\overset{(i)}{\underset{xx}{P^{\wedge}}}(f) = \frac{T_S}{K.M}\left|\sum_{n=0}^{\overset{\wedge}{M-1}} x_i(n)w(n).e^{-j2\pi fn}\right|^2 \tag{10}$$

The normalized frequency variable and the K normalized constant are defined in equation 10, where $w(n)$ represents the windowing function. The calculation of power spectral density estimation is performed using equation 12, with the value of K constant given in equation 11, as described by [6], [39], and [40].

$$K = \frac{1}{M}\sum_{n=0}^{M-1} w^2(n) \tag{11}$$

$$\overset{W}{\underset{xx}{P^{\wedge}}}(f) = \frac{1}{L}\sum_{i=0}^{\overset{\wedge}{L-1}} \overset{(i)}{\underset{xx}{P^{\wedge}}}(f) \tag{12}$$

III. FERRORESONANCE MODELING AND DATA ACQUISITION SYSTEM

Ferroresonance is a non-linear phenomenon that results in sudden voltage or current spikes, and it is commonly observed in long electric transmission lines [6], [41]. This chaotic behavior is a unique characteristic of the system. In this study, data collection was performed on the 380kV electrical energy grid in the Oymapinar-Seydisehir model in Turkey, as shown in Figure 1. The system design was modeled using MATLAB-Simulink©and actual transmission line parameters listed in Table 1 were incorporated. A schematic diagram of the power transmission line is also presented in Figure 1.

Figure 1 illustrates the schematic model of the Seydisehir-Oymapinar power transmission line, which is designed for the transmission of energy from the power generation source to the end-user. The model utilizes a symbolic representation to depict the various components of the transmission line. It is

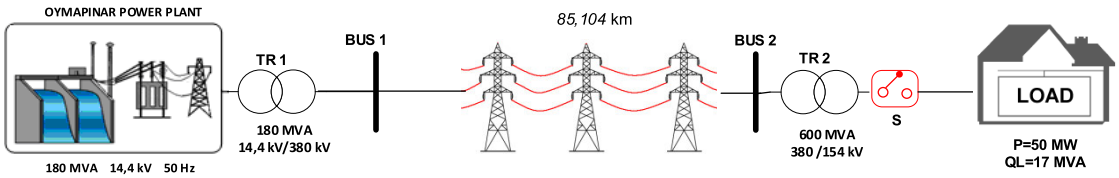

FIGURE 1. Schematic diagram of oymapinar-seydisehir electric power network in Turkey.

TABLE 1. Parameters of seyitomer-isiklar electric power network.

Electrical Components	*Parameters*
Generator	180 MVA, 14,4 kV, 50 Hz
Transformers	TR_1: 180 MVA, 14.4kV/380kV
	TR_2: 600kVA, 380kV/154kV
Lines	Pi Line (B1-B2): 85.104 km
	R: 0.2568 ohm/km
	L: 2e-3 H/km
	C: 8.6e-9 F/km
	Line (B2-B3): R:1 ohm, L:1e-3H
Loads	L_1:P=50MW, Qc=17MVAR
Switch	S: 2.5-5sec. - On
	0-2.5 sec. - Off

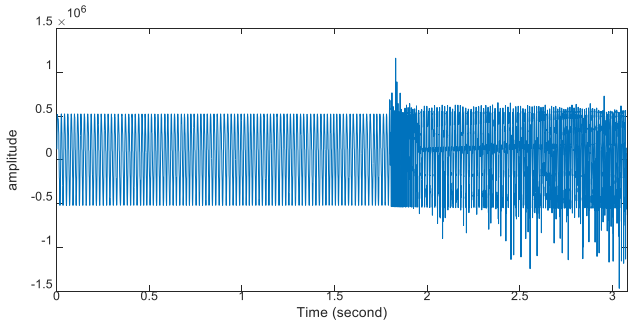

FIGURE 2. Time Voltage diagram on electric power line (including ferroresonance region.

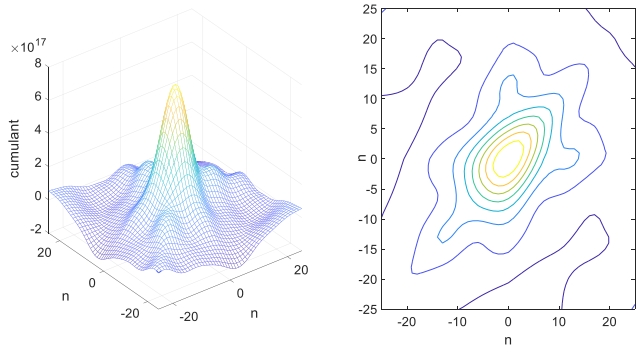

a) Three Dimensional Cumulant Analysis b) Contour Analysis

FIGURE 3. Third-order cumulant and contour analysis of ferroresonance phenomena.

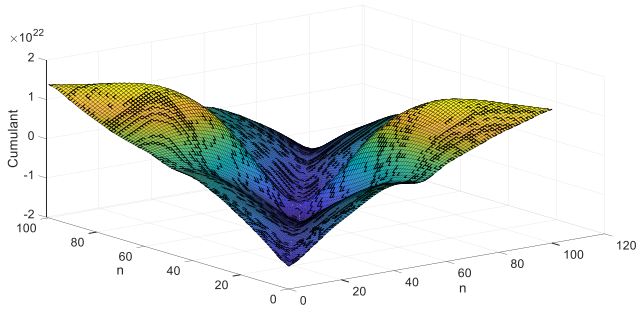

FIGURE 4. Fourth degree cumulant analysis of ferroresonance data.

noteworthy that this graphical representation was produced using Matlab Simulink, as reported previously in references 4 and 10, and is not featured in this article. Table 1 furnishes the electrical parameters of the power transmission line, encompassing its length and the symbolic representation of its interruption and switching points. Figure 2 illustrates the time-amplitude diagram resulting from the ferroresonance scenario implemented on the model.

Ferroresonance is a phenomenon that can cause excessive voltage fluctuations following a fault in power systems. A modeling approach has been developed to study ferroresonance and the resulting voltage fluctuations, as illustrated in Figure 2. Upon closer examination, the graph in Figure 2 exhibits classical ferroresonance behavior, which is characterized by ferromagnetic properties.

However, in this study, researchers have undertaken a detailed investigation of signal-based analysis techniques for the detection of ferroresonance.

IV. FEATURE EXTRACTION AND FERRORESONANCE ANALYSIS OF THE POWER NETWORK DATA

The phenomenon of ferroresonance in electrical power systems is a complex issue that can result in significant increases in voltage. In this particular study, real model parameters with a nominal voltage of 380 kV were employed to investigate the formation of ferroresonance and the resulting overvoltages that can exceed 1 MV. The analysis involved the use of two visualization techniques, namely a three-dimensional Cumulative analysis and a Contour plot, which are presented in Figures 3a and 3b, respectively.

The results reveal a clear observation of the highest voltage value due to ferroresonance in the graph. Specifically, the cumulant value of 4×10^{17} amplitude represents the peak value of the ferroresonance overvoltage.

These fidings demonstrate the potential danger associated with ferroresonance in electrical power systems, and underscore the importance of understanding and mitigating this

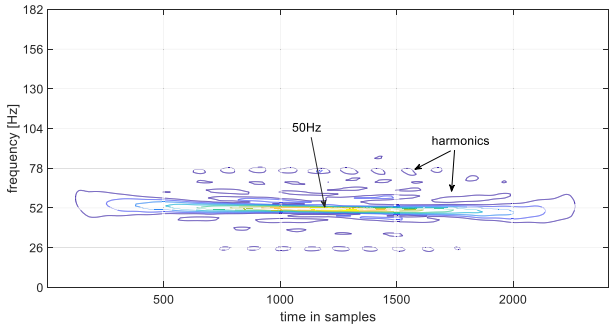

FIGURE 5. Wigner-Ville analysis for before ferroresonance.

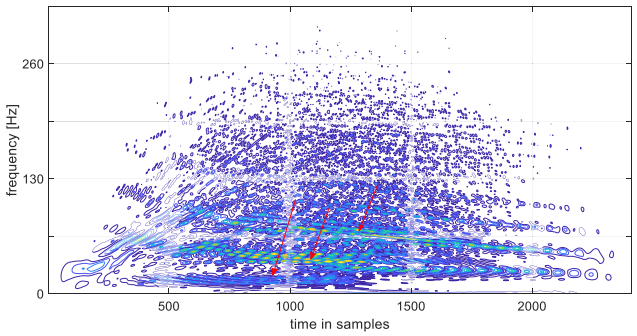

FIGURE 6. Wigner-Ville analysis for ferroresonance region.

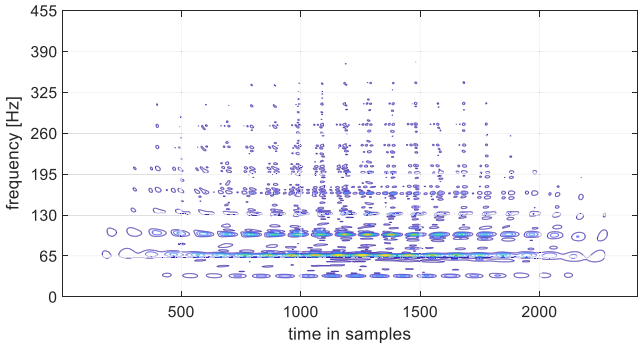

FIGURE 7. Wigner-Ville analysis for after ferroresonance.

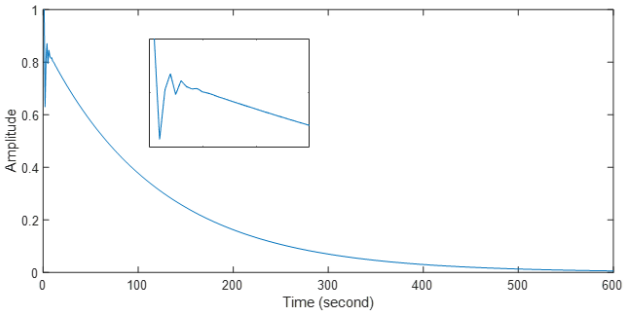

FIGURE 8. Unit impulse response of ferroresonance phenomena.

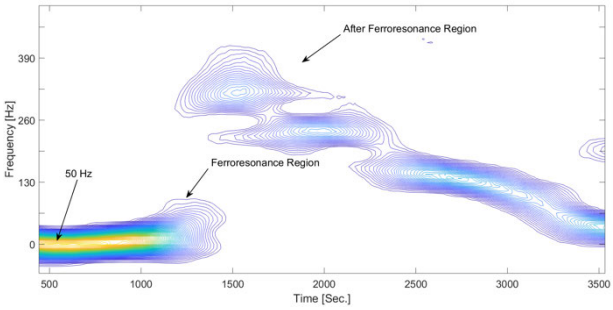

FIGURE 9. Spectrogram graphics of ferroresonance phenomenon.

phenomenon to ensure the safety and reliability of power systems.

The fourth-order cumulant analysis graph is depicted in Figure 4, where 'n' denotes the number of data. In practical settings, cumulant analysis is often conducted using a finite number of data points, and the resulting estimates are asymptotically unbiased.

Figure 5 displays the results of the wavelet-based windowed differentiation (WWD) analysis for the pre-ferroresonance interval. In this analysis, all ferroresonance data at 50 Hz is examined over a certain time period. Upon onset of ferroresonance, the intensity of the signal appears to increase. Prior to ferroresonance, the fundamental frequency of the system is 50 Hz, as depicted by the dominant spectral component. The yellow region in the figure corresponds to the ferroresonance region, which is also evident as a bifurcation in other analyses.

Figure 6 presents the outcomes of the wavelet-based time-frequency analysis performed in the ferroresonance region, where a well-defined peak featuring high amplitudes is observed at 50 Hz, 100 Hz, and 150 Hz. These frequency values can be identified as the fundamental frequency and its associated harmonics. The manifestation of destructive effects, along with their respective frequency components, can be observed in the ferroresonance region as a result of the underlying phenomenon. Moreover, the frequency is determined to attain a peak value of 650 Hz.

Figure 7 shows a simpler and more uniform distribution in the ferroresonance region following the occurrence of ferroresonance, as compared to the wavelet variance distribution (WV Distribution). Nonetheless, high amplitudes are observed at frequencies ranging from 50 Hz to approximately 100 Hz, with decreasing amplitude and density as the frequency increases. This distribution can be represented as a time-frequency distribution exhibiting the characteristics before and after the ferroresonance event.

The analysis of the ferroresonance signal in this model is demonstrated as the unit impulse response, which represents the output of a rigidity process, as shown in Figure 8. The impulse analysis of the ferroresonance phenomenon depicted in Figure 8 corresponds to the time-amplitude diagram presented in Figure 2. The collapse or damping of the phenomenon is demonstrated by zooming in on Figure 8.

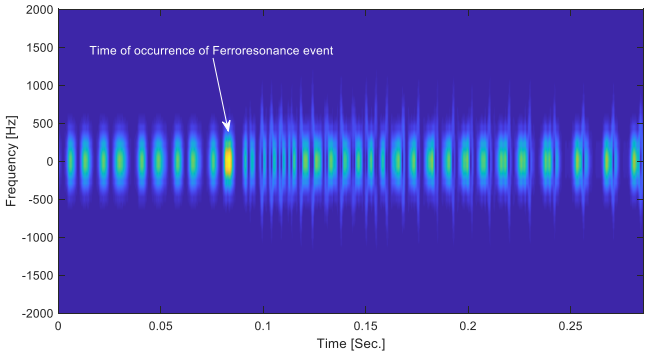

FIGURE 10. Spectrogram Analysis of ferroresonance phenomena.

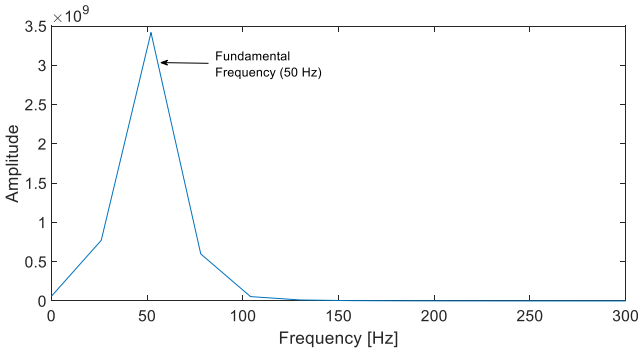

FIGURE 11. Frequency-Power analysis for before ferroresonance.

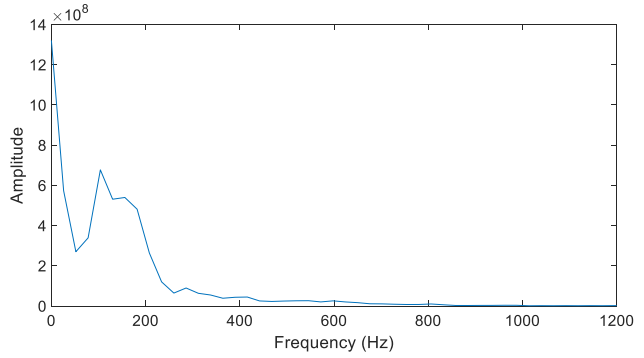

FIGURE 12. Frequency-Power analysis for ferroresonance region.

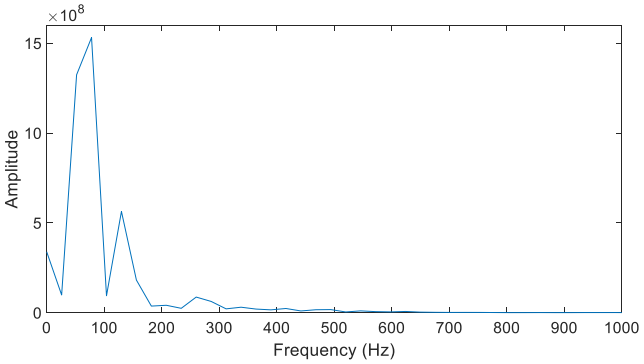

FIGURE 13. Frequency-Power analysis for after ferroresonance.

In Figure 9, the Spectrogram graph of the ferroresonance phenomena is presented. The basic frequency of the system, 50Hz, is clearly visible on the graph. At around 1500 sample numbers, there is a transition in the frequency from 250Hz to a lower frequency, as the graph breaks down (the moment of ferroresonance) and continues to decrease. The detection of ferroresonance phenomena can be observed as this transition occurs.

Unlike Figure 9, another Spectrogram graph with different window and resolution is presented in Figure 10. In this representation, low-amplitude frequency values of 50 Hz are seen prior to ferroresonance, whereas high-amplitude values are seen during ferroresonance.

Additionally, it can be observed that the frequency values lose their coherence with the mains frequency and exhibit scattering both during and after ferroresonance. Please note that while the time axis has been zoomed in on the data, it does not reflect the actual time duration of the data.

Figure 11 shows a power graph of around 3.4×10^9 at 50Hz base frequency value before ferroresonance.

Figure 10 presents a spectrogram that delineates the alterations in frequency before and after the onset of ferroresonance, whereas Figure 12 exhibits a power graph with a fundamental frequency of 50 Hz and an approximate value of 3.4×10^9 prior to the occurrence of ferroresonance, thereby enabling precise identification of the moment at which ferroresonance transpires.

The analysis presented in Figure 12 indicates that during the occurrence of ferroresonance, the frequency-power diagram exhibits a highly variable structure with a lower amplitude level. There is a sharp decline in the power amplitude, followed by a slight increase up to 400 Hz.

Figure 13 illustrates the before/after-ferroresonance graph, which exhibits variable frequency fluctuation ranging between 0 and 650 Hz. This implies that the dampening effect of the ferroresonance phenomenon persists even after its occurrence. It can be inferred that the network operates in an insecure manner with frequency fluctuations after the event of ferroresonance.

The frequency-power relationship of the entire system is depicted in Figure 14. The graph illustrates the variations in frequency-power before, during, and after the occurrence of ferroresonance. During the pre-ferroresonance phase, the electrical network exhibits a 50Hz fundamental frequency with an amplitude value of 2.3×10^9. However, during the ferroresonance event, the current level decreases, leading to high frequencies and low amplitude powers. After the ferroresonance, the system experiences a collapse, resulting in sustained low amplitude powers at high frequencies.

V. DISSCUSSION

The analysis of ferroresonance events using signal processing techniques, such as Wavelet, FFT, and DFT, can provide

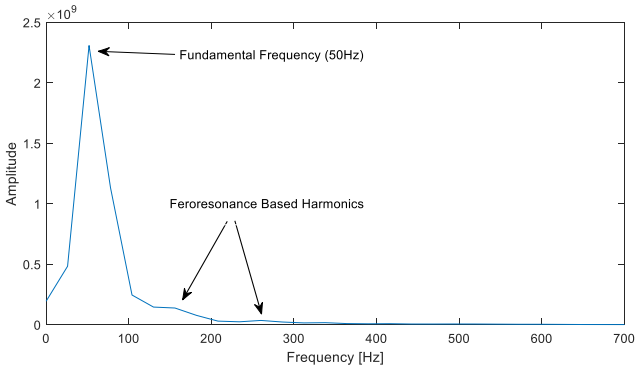

FIGURE 14. Frequency-Power analysis of the system (all).

valuable insights into the frequency components present in the signal [4], [42]. These techniques enable the conversion of the time-domain signal into its frequency-domain representation, which is useful for identifying the frequency components responsible for the ferroresonance.

Spectrum analysis is another technique that can be used to identify frequency components in the signal. It provides a graphical representation of the signal in the frequency domain, enabling the identification of the frequency components present in the signal [4], [42].

Wigner Ville analysis is a time-frequency analysis technique that can provide more detailed insights into the frequency components present in the signal. It provides a time-frequency representation of the signal, which enables the identification of frequency components that may vary over time. This can be particularly useful for analyzing non-stationary signals, such as those seen in ferroresonance events [10], [43].

High-resolution spectral analysis is another technique that can provide more precise identification of closely spaced frequency components. This technique enables identification of frequency components that may be difficult to discern with FFT or DFT analysis [44], [45].

In determining the ferroresonance condition, the contributions of Wigner Ville and high-resolution analysis lie in their ability to provide more detailed and precise information regarding the frequency components present in the signal. This can enable more accurate identification of the ferroresonance condition and a better understanding of its behaviour.

Compared to FFT and DFT analysis, Wigner Ville analysis provides a more precise time-frequency representation of the signal, allowing for the identification of frequency components that vary over time. This technique can also identify frequency components that are closely spaced together, which may be difficult to differentiate with FFT or DFT analysis alone. Additionally, Wigner Ville analysis can provide information on the time evolution of frequency components, which can be useful in understanding the dynamics of the ferroresonance event [46].

Overall, the use of signal processing techniques such as Wavelet, FFT, DFT, spectrum analysis, Wigner Ville analysis, and high-resolution spectral analysis can provide valuable insights into the ferroresonance event. The choice of which technique to use may depend on the specific characteristics of the signal being analyzed and the information required for the analysis. However, Wigner Ville analysis can provide a more detailed and precise time-frequency representation of the signal, making it a valuable technique for analyzing ferroresonance events [47], [48].

It should be noted that the advantages of Wigner Ville analysis are its ability to provide a high-resolution time-frequency representation of the signal, with the ability to distinguish between closely spaced frequency components, and its ability to capture time-frequency localization of the signal. Moreover, Wigner Ville analysis provides a representation of the signal that is not limited by the uncertainty principle, as in FFT or DFT analysis. Therefore, Wigner Ville analysis can provide a more complete and accurate understanding of the ferroresonance event.

VI. CONCLUSION

This study has investigated the phenomena of ferroresonance using High-Order Spectral Analysis (HOSA) methods. The results demonstrate that HOSA can provide a comprehensive analysis of the nonlinear aspects of ferroresonance in electrical systems. The study has shown that the use of higher-order moments and cumulants in HOSA can offer better results in analyzing non-Gaussian and non-stationary processes, which are difficult to analyze using traditional methods. Additionally, the Wigner-Ville Distribution (WVD) approach has been employed in this study to provide a detailed understanding of the energy spectrum in terms of instant power and frequency in time, as well as the total energy of the signal in the time-frequency plane. The findings of this study contribute to a better understanding of the causes and prevention of ferroresonance in electrical power transmission lines, which is important for maintaining the efficiency, reliability, and safety of power systems.

In future research concerning the analysis of ferroresonance using automated algorithms for detecting and classifying ferroresonance events using Wigner-Ville and HOSA techniques could be developed, incorporating machine learning algorithms to train models on large datasets of ferroresonance signals and accurately predict its occurrence in real-time.

REFERENCES

[1] M. J. Burke and J. C. Stephens, "Political power and renewable energy futures: A critical review," *Energy Res. Social Sci.*, vol. 35, pp. 78–93, Jan. 2018, doi: 10.1016/j.erss.2017.10.018.

[2] B. Matek and K. Gawell, "The benefits of baseload renewables: A misunderstood energy technology," *Electr. J.*, vol. 28, no. 2, pp. 101–112, Mar. 2015, doi: 10.1016/j.tej.2015.02.001.

[3] J. A. Laghari, H. Mokhlis, A. H. A. Bakar, and H. Mohamad, "Application of computational intelligence techniques for load shedding in power systems: A review," *Energy Convers. Manage.*, vol. 75, pp. 130–140, Nov. 2013, doi: 10.1016/j.enconman.2013.06.010.

[4] T. C. Akinci, N. Ekren, S. Seker, and S. Yildirim, "Continuous wavelet transform for ferroresonance phenomena in electric power systems," *Int. J. Electr. Power Energy Syst.*, vol. 44, no. 1, pp. 403–409, Jan. 2013, doi: 10.1016/j.ijepes.2012.07.001.

[5] N. A. Sabiha and H. I. Alkhammash, "Ferroresonance overvoltage mitigation using surge arrester for grid-connected wind farm," *Intell. Autom. Soft Comput.*, vol. 31, no. 2, pp. 1107–1118, 2022, doi: 10.32604/iasc.2022.020070.

[6] O. Akgun, "Analysis of heart sound signals in mitral valve diseases," Ph.D. dissertation, Dept. Electron. Commun., Inst. Pure Appl. Sci., Marmara Univ., Istanbul, Turkey, 2011.

[7] B. A. Carreras, V. E. Lynch, I. Dobson, and D. E. Newman, "Critical points and transitions in an electric power transmission model for cascading failure blackouts," *Chaos, Interdiscipl. J. Nonlinear Sci.*, vol. 12, no. 4, pp. 985–994, Dec. 2002, doi: 10.1063/1.1505810.

[8] I. Kazhekin and M. Kharitonov, "Prevention of ferroresonant processes in microgrid operating in island mode," in *Energy Ecosystems: Prospects and Challenges*. Cham, Switzerland: Springer, 2023, pp. 86–94, doi: 10.1007/978-3-031-24820-7_8.

[9] R. M. Larik, M. W. Mustafa, and M. N. Aman, "A critical review of the state-of-art schemes for under voltage load shedding," *Int. Trans. Electr. Energy Syst.*, vol. 29, no. 5, p. e2828, Jan. 2019, doi: 10.1002/2050-7038.2828.

[10] Ö. Akgün, T. Ç. Akıncı, G. Erdemir, and S. Şeker, "Analysis of instantaneous frequency, instantaneous amplitude and phase angle of ferroresonance in electrical power networks," *J. Electr. Eng.*, vol. 70, no. 6, pp. 494–498, Dec. 2019, doi: 10.2478/jee-2019-0084.

[11] M. Kutija and L. Pravica, "Effect of harmonics on ferroresonance in low voltage power factor correction system—A case study," *Appl. Sci.*, vol. 11, no. 10, p. 4322, May 2021, doi: 10.3390/app11104322.

[12] G. B. Gharehpetian, A. Yazdani, and B. Zaker, *Power System Transients*. Boca Raton, FL, USA: CRC Press, 2023.

[13] A. Djebli, F. Aboura, L. Roubache, and O. Touhami, "Impact of the eddy current in the lamination on ferroresonance stability at critical points," *Int. J. Electr. Power Energy Syst.*, vol. 106, pp. 311–319, Mar. 2019, doi: 10.1016/j.ijepes.2018.10.008.

[14] S. Boutora and H. Bentarzi, "Ferroresonance study using false trip root cause analysis," *Energy Proc.*, vol. 162, pp. 306–314, Apr. 2019, doi: 10.1016/j.egypro.2019.04.032.

[15] Ł. Majka and M. Klimas, "Diagnosis of a ferroresonance type through visualisation," in *Proc. ITM Web Conf.*, vol. 28, 2019, p. 01039, doi: 10.1051/itmconf/20192801039.

[16] A. Rezaei-Zare, A. H. Etemadi, and R. Iravani, "Challenges of power converter operation and control under ferroresonance conditions," *IEEE Trans. Power Del.*, vol. 32, no. 6, pp. 2380–2388, Dec. 2017, doi: 10.1109/TPWRD.2016.2626266.

[17] M. Yang, W. Sima, P. Duan, M. Zou, D. Peng, Q. Yang, and Q. Duan, "Electromagnetic transient study on flexible control processes of ferroresonance," *Int. J. Electr. Power Energy Syst.*, vol. 93, pp. 194–203, Dec. 2017, doi: 10.1016/j.ijepes.2017.05.026.

[18] W. Kraszewski, P. Syrek, and M. Mitoraj, "Methods of ferroresonance mitigation in voltage transformers in a 30 kV power supply network," *Energies*, vol. 15, no. 24, p. 9516, Dec. 2022, doi: 10.3390/en15249516.

[19] S. R. Naidu and B. A. Souza, "Analysis of ferroresonant circuits in the time and frequency domains," *IEEE Trans. Magn.*, vol. 33, no. 5, pp. 3340–3342, Sep. 1997.

[20] Ł. Majka and M. Klimas, "Diagnostic approach in assessment of a ferroresonant circuit," *Electr. Eng.*, vol. 101, no. 1, pp. 149–164, Apr. 2019.

[21] A. Naberezhnykh, D. Ingram, and I. Ashton, "Wavelet applications for turbulence characterisation of real tidal flows measured with an ADCP," *Ocean Eng.*, vol. 270, Feb. 2023, Art. no. 113616, doi: 10.1016/j.oceaneng.2022.113616.

[22] J. A. Corea-Araujo, F. González-Molina, J. A. Martínez, J. A. Barrado-Rodrigo, and L. Guasch-Pesquer, "Tools for characterization and assessment of ferroresonance using 3-D bifurcation diagrams," *IEEE Trans. Power Del.*, vol. 29, no. 6, pp. 2543–2551, Dec. 2014, doi: 10.1109/TPWRD.2014.2320599.

[23] C. L. Nikias and J. M. Mendel, "Signal processing with higher-order spectra," *IEEE Signal Process. Mag.*, vol. 10, no. 3, pp. 10–37, Jul. 1993, doi: 10.1109/79.221324.

[24] K. Sweitzer, N. Bishop, and V. Genberg, "Efficient computation of spectral moments for determination of random response statistics," in *Proc. ISM*, vol. 2004, 2004, pp. 2677–2692.

[25] B. Boashash, "Note on the use of the Wigner distribution for time-frequency signal analysis," *IEEE Trans. Acoust., Speech, Signal Process.*, vol. ASSP-36, no. 9, pp. 1518–1521, Sep. 1988, doi: 10.1109/29.90380.

[26] J. O'Toole, M. Mesbah, and B. Boashash, "A discrete time and frequency Wigner–Ville distribution: Properties and implementation," in *Proc. Int. Conf. Digital Signal Process. Commun. Syst.*, vol. 400, 2005, pp. 19–21.

[27] T. A. C. M. Claasen, "The Wigner distribution—A tool for time-frequency signal analysis," *Philips J. Res.*, vol. 35, pp. 217–250, Jan. 1980.

[28] I. M. Zoukaneri and M. J. Porsani, "High-resolution time frequency analysis using Wigner–Ville distribution and the maximum entropy method: Application for gas and hydrates identification," in *Proc. 13th Int. Congr. Brazilian Geophys. Soc.*, Aug. 2013, pp. 957–961.

[29] E. Chassande-Mottin and A. Pai, "Discrete time and frequency Wigner–Ville distribution: Moyal's formula and aliasing," *IEEE Signal Process. Lett.*, vol. 12, no. 7, pp. 508–511, Jul. 2005.

[30] S. Akhavan, M. A. Akhaee, and S. Sarreshtedari, "Images steganalysis using GARCH model for feature selection," *Signal Process., Image Commun.*, vol. 39, pp. 75–83, Nov. 2015, doi: 10.1016/j.image.2015.08.006.

[31] B. Boashash, *Time-Frequency Signal Analysis and Processing*. New York, NY, USA: Academic, 2015.

[32] M. Yang, W. Sima, L. Chen, P. Duan, P. Sun, and T. Yuan, "Suppressing ferroresonance in potential transformers using a model-free active-resistance controller," *Int. J. Electr. Power Energy Syst.*, vol. 95, pp. 384–393, Feb. 2018, doi: 10.1016/j.ijepes.2017.08.035.

[33] F. Hlawatsch and P. Flandrin, "The interference structure of the Wigner distribution and related time-frequency signal representations," in *The Wigner Distribution: Theory and Applications in Signal Processing*. Amsterdam, The Netherlands: Elsevier, 1997, pp. 59–133.

[34] A. J. Janssen, "Gabor representation and Wigner distribution of signals," in *Proc. IEEE Int. Conf. Acoust., Speech, Signal Process.*, vol. 9, Mar. 1984, pp. 258–261.

[35] A. J. E. M. Janssen, "The Zak transform: A signal transform for sampled time-continuous signals," *Philips J. Res.*, vol. 43, no. 1, pp. 23–69, 1988.

[36] L. Debnath, "Recent developments in the Wigner–Ville distribution and time-frequency signal analysis," in *Proc. Indian Nat. Sci. Acad., A*, vol. 68, pp. 35–56, Jan. 2002.

[37] P. D. Welch, "A direct digital method of power spectrum estimation," *IBM J. Res. Develop.*, vol. 5, no. 2, pp. 141–156, Apr. 1961, doi: 10.1147/rd.52.0141.

[38] P. Welch, "The use of fast Fourier transform for the estimation of power spectra: A method based on time averaging over short, modified periodograms," *IEEE Trans. Audio Electroacoustics*, vol. AE-15, no. 2, pp. 70–73, Jun. 1967.

[39] L. C. Caldas and L. A. Baccalá. (2016). *Power Spectral Density (PSD) Estimation: MATLAB Algorithm Implementation for Array Signal Processing and Test Validation*. [Online]. Available: https://www.researchgate.net/publication/296962602_Power_spectral_density_PSD_estimation_MATLAB_algorithm_implementation_for_array_signal_processing_and_test_validation

[40] A. Krishna and J. Andrews, "PSD computation using modified Welch algorithm," *Int. J. Sci. Res. Eng. Technol.*, vol. 4, no. 9, pp. 951–954, 2015.

[41] H. Zhang, W. Sima, and M. Yang, "A data-driven approach for electromagnetic transient recognition using transfer learning," *CSEE J. Power Energy Syst.*, vol. 2023, pp. 1–11, Jan. 2023, doi: 10.17775/CSEEJPES.2021.05660.

[42] R. Martinez, A. Arroyo, A. Pigazo, M. Manana, E. Bayona, F. J. Azcondo, S. Bustamante, and A. Laso, "Acoustic noise-based detection of ferroresonance events in isolated neutral power systems with inductive voltage transformers," *Sensors*, vol. 23, no. 1, p. 195, Dec. 2022, doi: 10.3390/s23010195.

[43] S. Seker, T. C. Akinci, and S. Taskin, "Spectral and statistical analysis for ferroresonance phenomenon in electric power systems," *Electr. Eng.*, vol. 94, no. 2, pp. 117–124, Jun. 2012, doi: 10.1007/s00202-011-0224-4.

[44] M. F. Wahab and T. C. O'Haver, "Peak deconvolution with significant noise suppression and stability using a facile numerical approach in Fourier space," *Chemometric Intell. Lab. Syst.*, vol. 235, Apr. 2023, Art. no. 104759, doi: 10.1016/j.chemolab.2023.104759.

[45] H. Lim, Y. H. Lee, S. S. Bang, and Y. Shin, "Application of enhanced optimal-detection of time–frequency domain reflectometry on HTS cable with high-resolution," *IEEE Trans. Appl. Supercond.*, vol. 33, no. 5, pp. 1–10, Aug. 2023, doi: 10.1109/TASC.2023.3237126.

[46] K. Solak, W. Rebizant, and M. Kereit, "Detection of ferroresonance oscillations in medium voltage networks," *Energies*, vol. 13, no. 16, p. 4129, Aug. 2020, doi: 10.3390/en13164129.
[47] N. A. Khan and M. Sandsten, "Time–frequency image enhancement based on interference suppression in Wigner–Ville distribution," *Signal Process.*, vol. 127, pp. 80–85, Oct. 2016, doi: 10.1016/j.sigpro.2016.02.027.
[48] M. Sandsten. *Time-Frequency Analysis of Time-Varying Signals and Non-Stationary Processes*. Accessed: May 2023. [Online]. Available: https://www.maths.lu.se/fileadmin/maths/personal_staff/mariasandsten/TFkompver4.pdf

TAHIR CETIN AKINCI (Senior Member, IEEE) received the bachelor's degree in electrical engineering, in 2000, and the master's and Ph.D. degrees, in 2005 and 2010, respectively. From 2003 to 2010, he was a Research Assistant with Marmara University, Istanbul, Turkey. He is currently a Full Professor with the Electrical Engineering Department, Istanbul Technical University (ITU). He assumed the role of a Visiting Scholar with the University of California at Riverside (UCR). His research interests include artificial neural networks, deep learning, machine learning, cognitive systems, signal processing, and data analysis. In 2022, he was honored with the International Young Scientist Excellence Award as well as the Best Researcher Award for his exceptional research achievements.

OMER AKGUN received the first Ph.D. degree in communication engineering from Yildiz Technical University, in 2009, and the second Ph.D. degree from the Electronic and Communication Education Department, Marmara University, in 2011. He is currently an Assistant Professor with the Department of Computer Engineering, Faculty of Technology, Marmara University. His current research interests include signal processing, biomedical signal processing, signal modeling, and communication systems.

MUSA YILMAZ (Senior Member, IEEE) received the B.S., M.S., and Ph.D. degrees in electrical and electronics engineering, in 2001, 2004, and 2013, respectively.

From 2004 to 2014, he was with Dicle University, Diyarbakı, Turkey. Since 2014, he has been an Assistant Professor with the Electrical and Electronics Engineering Department, Batman University. In 2015 and 2016, he was a Visiting Scholar with the University of California at Los Angeles (UCLA). Since 2022, he has been a Visiting Scholar with the University of California at Riverside (UCR). He is currently a Partner with Biosys LLC. His research interests include smart grids, renewable energy, power systems, artificial neural networks, deep learning, machine learning, signal processing, and data analysis.

Dr. Yılmaz served as the Editor-in-Chief for the *Balkan Journal of Electrical and Computer Engineering* (BAJECE) and the *European Journal of Technique* (EJT).

ALFREDO A. MARTINEZ-MORALES received the B.S., M.S., and Ph.D. degrees in electrical engineering from the University of California at Riverside (UCR), in 2005, 2008, and 2010, respectively. He is currently the Managing Director of the Southern California Research Initiative for Solar Energy (SC-RISE) and holds the position of Research Professor with the Bourns College of Engineering, Center for Environmental Research and Technology (CE-CERT). He also plays a key role as a Principal Investigator with the Sustainable Integrated Grid Initiative (SIGI) and the Distributed Energy Resources Laboratory (DERL), UCR, contributing to the engineering, permitting, and deployment of microgrids throughout Southern California. His current research interests include solar cells, alkali metal ion batteries, highly integrated renewables, energy storage systems, and microgrids.